

## **Supplementary Material for**

### **Reduced BOLD connectivity is related to hypoperfusion in Alzheimer's disease**

by Jens Göttler, Christine Preibisch, Isabelle Riederer, Lorenzo Pasquini, Panagiotis Alexopoulos, Karl Peter Bohn, Igor Yakushev, Ebba Beller, Stephan Kaczmarz, Claus Zimmer, Timo Grimmer, Alexander Drzezga, and Christian Sorg

#### **Content table:**

##### Supplementary Methods

- Voxel-based morphometry preprocessing

- FMRI preprocessing

##### Supplementary Results

- Correlation of voxel-wise CBF and rFDG-uptake

- Comparison of results for patients with early and late onset AD

##### References

## Supplementary Methods:

### Voxel-based morphometry preprocessing.

We used the VBM8 toolbox (<http://dbm.neuro.uni-jena.de/vbm.html>) applying default parameters to analyse grey matter density within the DMN as we previously described in detail.<sup>1</sup> Images were bias-corrected, registered using linear (i.e., 12-parameter affine registration) and non-linear (i.e., warping regularization) transformations and tissue classified. Subsequently, grey and white matter segments were modulated to account for volume changes that result from the normalization process using DARTEL in order to locally preserve actual grey and white matter values. Afterwards, images were smoothed with a FWHM Gaussian kernel of 8x8x8mm.

### FMRI preprocessing

Before fMRI preprocessing the first three images of each subject's EPI-time-series were discarded. Remaining EPI images were aligned to the anterior-posterior commissure and slice time corrected to account for differences in slice acquisition time using SPM12. Afterwards, images were realigned to the subject's mean EPI to correct for head motion during the fMRI scan and co-registered to the individual MP-RAGE image using a six parameter rigid-body transformation. Each subject's brain data were then normalized to the MNI standard template and smoothed with a full width at half maximum (FWHM) Gaussian kernel of 8x8x8mm. MNI tissue-probability maps of grey matter, white matter, and cerebrospinal fluid were warped onto single-subject MP-RAGE images. Excessive head motion (maximal translation or rotation  $> 3\text{mm}$  or  $3^\circ$  and mean translation or rotation  $> 0.15\text{mm}$  or  $0.1^\circ$  relative to the previous volume) was applied as an exclusion criterion. Three patients with AD and two healthy controls had to be excluded due to excessive movement. Furthermore, we critically controlled for potential movement artefacts, following<sup>2</sup>. Two sample *t*-tests yielded no significant differences between groups regarding translational and rotational head movements of any direction. In the same way, root mean square of the translational and rotational head movement parameters was not different across groups.

Preprocessed fMRI data of all subjects were concatenated and entered into an independent component analysis (ICA) with a group-ICA framework<sup>3</sup> using the GIFT toolbox (Medical Imaging Analysis Lab, The Mind Research Network; <http://icatb.sourceforge.net>). Dimensionality estimation was performed using minimum description length algorithm,

resulting in a mean estimate of 16 components. Only the most stable ICs with a stability index  $>0.9$  were identified by iteratively running 30 independent component analyses using the ICASSO procedure<sup>4</sup> and were subsequently back-reconstructed into single-subject space. For each subject, each component resulted in a spatial map reflecting that component's z-scored spatial BOLD-FC pattern. To automatically select the DMN we ran a spatial multiple regression of all independent components on a DMN template derived from a previous study (available online at <http://fsl.fmrib.ox.ac.uk/analysis/brainmap+rsns/>).<sup>5</sup> The independent component with the highest spatial correlation ( $R = 0.44$ ) and focus on the posterior brain was used for further analysis as proxy for the pDMN. Accordingly, we chose the PVN as a control network.

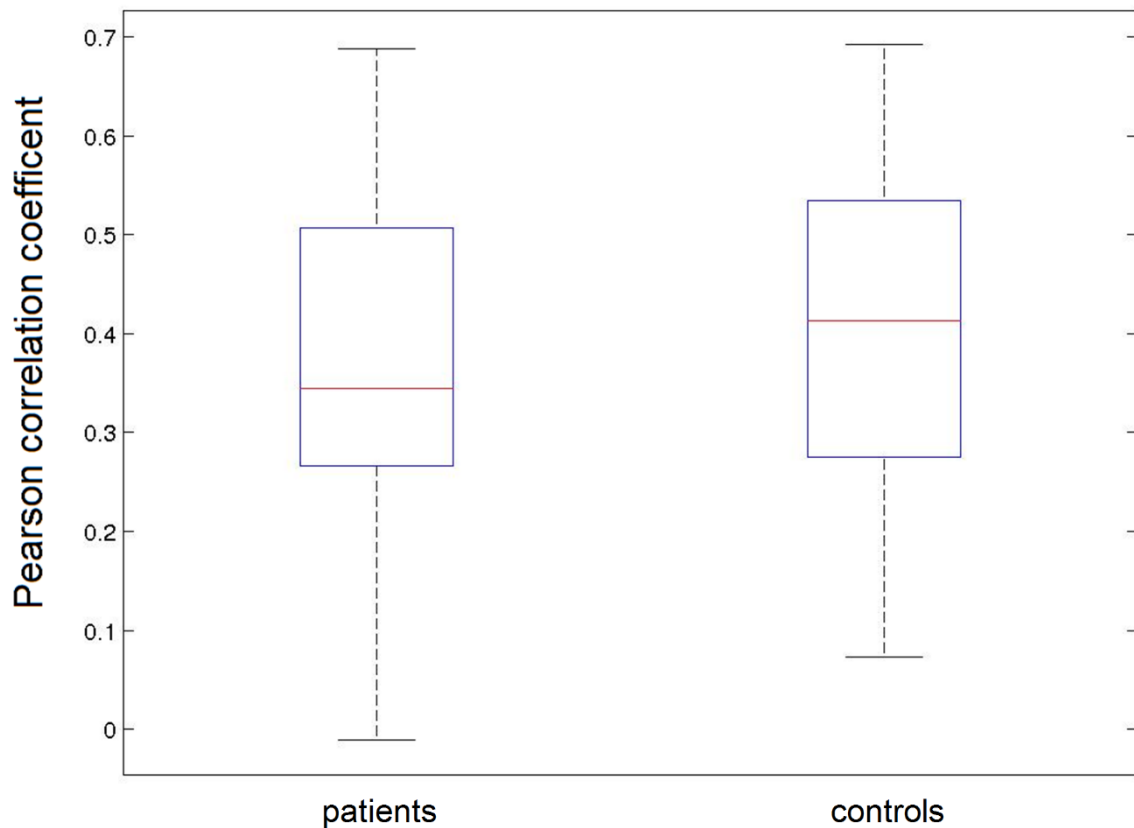
## Supplementary Results

### Correlation of voxel-wise CBF and rFDG-uptake

No significant correlation of averaged values of CBF and rFDG-uptake within the pDMN were observed across patients. However, several previous PET-based studies have shown that both measures are highly correlated,<sup>6</sup> and FDG-uptake is perfusion dependent itself (see e.g. <sup>7,8</sup>). To investigate whether both measures were associated on a voxel-level, CBF and rFDG-uptake values of normalized, unsmoothed data were correlated in the individual GM masks within the pDMN in each subject using a MATLAB based script. Indeed, CBF and rFDG-uptake were significantly correlated on a voxel-level within subjects (median individual Pearson correlation coefficients of patients/controls  $r=0.345/0.414$ ; Supplement Figure 1) with no significant group difference being observed (two-sample t-test:  $p=0.483$ ). This is a contradiction at first view to our finding of not-correlated mean CBF and mean rFDG-uptake. However, the two correlation approaches assess different aspects of associations between two variables, i.e. the rate of change in the voxel-wise comparison and the inter-subject variability in the comparison of averaged levels across subjects, respectively. Therefore, the two modalities do not necessarily have to be linked in both cases. Indeed, our finding of voxel-wise correlations in the presence of absent associations of averaged levels of CBF and FDG-uptake has also been described previously by Cha et al. in healthy subjects.<sup>9</sup> They demonstrated considerably dissociated correlations between CBF and FDG-uptake, i.e. positive correlations across voxels and absent correlations across subjects in the parietal and occipital lobe as well as the cingulum (where our analyses focused on). However, they also found consistent positive voxel-wise and averaged correlations in the frontal and temporal lobes, and the striatum. In the hippocampus and amygdala, in contrast, neither voxel-wise nor averaged correlations have been observed. This high regional variability may partially be explained by the different physiological processes each modality depicts; ASL is mainly an extracellular signal with a temporal scale of few seconds, highly depending on the post-label delay (time between labeling the neck vessels and cerebral read-out), FDG-uptake on the other hand is an intracellular signal and acquired over 30-60 minutes. Furthermore, also a variable neurovascular coupling across brain regions and across subjects can account for the observed conflicting correlations of voxel-wise and averaged values, as measures are only locally and relatively associated.<sup>10</sup>

Concerning our study, we regressed out the mean FDG-uptake level of the whole network connectivity and subsequently compared the mean BOLD-residuals with the network's averaged perfusion level. By this approach, the relationship of the integrity of the whole

network and level of network perfusion, independent from the level of glucose metabolism is addressed. Complementary, to reveal spatial specificity within the pDMN, we only replaced mean-BOLD-FC by voxel-wise BOLD-FC but with the same explanatory mean-variables as conservative proxies for voxel-wise CBF and FDG-uptake.



**Supplement Figure 1: Voxel-wise spatial correlation of CBF and rFDG-uptake within the pDMN.** Boxplots illustrate individual (i.e. single subject) correlation coefficients for both groups. The boxes contain all values between the first and third quartile, the red line inside marks the median and the whiskers reach from minimum to maximum. Median individual Pearson correlation coefficients of patients/controls were  $r=0.345/0.414$ . No significant group difference has been observed (two-sample t-test:  $p=0.483$ ).

### **Comparison of results for patients with early and late onset AD**

We performed a control analysis to investigate whether patients with early onset AD (EOAD, <65years), who often suffer from autosomal dominant AD and whose pDMN BOLD-FC might be more affected, drive our results.<sup>11</sup> 14 patients were identified with EOAD, 18 with late onset AD (LOAD). First, we compared both groups' BOLD-FC by a two-sample t-test, which yielded no significant group differences. Averaged BOLD-FC within the DMN was not significantly different in EOAD ((mean BOLD-FC = 1.47) and LOAD (mean BOLD-FC = 1.43); two-sample t-test:  $p=0.740$ ). When comparing voxel-wise BOLD-FC with the control group, LOAD showed even more significant clusters of reduced BOLD-FC in the PCC/precuneus and inferior parietal lobule ( $\sum N=179$ ) compared to EOAD ( $\sum N=73$ ). We further conducted the ANCOVA model for EOAD & controls and LOAD & controls separately. Here, significant (and trend to significant) effects of group ( $p=0.031$ ) and group\*mean CBF ( $p=0.059$ ) have only been found in the LOAD & controls analysis. In the EOAD & controls group, p-values for the observed effects were  $p=0.196$  for the factor group, and  $p=0.143$  for factor group\*mean CBF.

In summary, we found no differences in BOLD-FC of the DMN in EOAD and LOAD. Separate ANCOVA analysis showed that results are rather driven by LOAD, maybe also because of the larger statistical power ( $N(\text{LOAD})=18$ ,  $N(\text{EOAD})=14$ ). However, we can exclude that EOAD individuals are the major contributors to the reported results.

## References

1. Koch K, Myers NE, Gottler J, et al. Disrupted Intrinsic Networks Link Amyloid-beta Pathology and Impaired Cognition in Prodromal Alzheimer's Disease. *Cerebral cortex* 2014.
2. Van Dijk KR, Sabuncu MR, Buckner RL. The influence of head motion on intrinsic functional connectivity MRI. *NeuroImage* 2012;59:431-438.
3. Calhoun VD, Adali T, Pearlson GD, Pekar JJ. Spatial and temporal independent component analysis of functional MRI data containing a pair of task-related waveforms. *Human brain mapping* 2001;13:43-53.
4. Himberg J, Hyvarinen A, Esposito F. Validating the independent components of neuroimaging time series via clustering and visualization. *NeuroImage* 2004;22:1214-1222.
5. Smith SM, Fox PT, Miller KL, et al. Correspondence of the brain's functional architecture during activation and rest. *Proceedings of the National Academy of Sciences of the United States of America* 2009;106:13040-13045.
6. Paulson OB, Hasselbalch SG, Rostrup E, Knudsen GM, Pelligrino D. Cerebral blood flow response to functional activation. *Journal of cerebral blood flow and metabolism : official journal of the International Society of Cerebral Blood Flow and Metabolism* 2010;30:2-14.
7. van Golen LW, RG IJ, Huisman MC, et al. Cerebral blood flow and glucose metabolism in appetite-related brain regions in type 1 diabetic patients after treatment with insulin detemir and NPH insulin: a randomized controlled crossover trial. *Diabetes care* 2013;36:4050-4056.
8. Alf MF, Duarte JM, Schibli R, Gruetter R, Kramer SD. Brain glucose transport and phosphorylation under acute insulin-induced hypoglycemia in mice: an 18F-FDG PET study. *Journal of nuclear medicine : official publication, Society of Nuclear Medicine* 2013;54:2153-2160.
9. Cha YH, Jog MA, Kim YC, Chakrapani S, Kraman SM, Wang DJ. Regional correlation between resting state FDG PET and pCASL perfusion MRI. *Journal of cerebral blood flow and metabolism : official journal of the International Society of Cerebral Blood Flow and Metabolism* 2013;33:1909-1914.
10. Whittaker JR, Driver ID, Bright MG, Murphy K. The absolute CBF response to activation is preserved during elevated perfusion: Implications for neurovascular coupling measures. *NeuroImage* 2016;125:198-207.
11. Chhatwal JP, Schultz AP, Johnson K, et al. Impaired default network functional connectivity in autosomal dominant Alzheimer disease. *Neurology* 2013;81:736-744.